Fermi National Accelerator Laboratory

FERMILAB-Pub-97/171-E
CDF

Limits on Quark-Lepton Compositeness Scales from Dileptons Produced in 1.8 TeV $p\bar{p}$ Collisions

F. Abe et al.
The CDF Collaboration

Fermi National Accelerator Laboratory
P.O. Box 500, Batavia, Illinois 60510

June 1997

Submitted to *Physical Review Letters*

Operated by Universities Research Association Inc. under Contract No. DE-AC02-76CH03000 with the United States Department of Energy

Limits on Quark-Lepton Compositeness Scales from Dileptons Produced in 1.8 TeV $p\bar{p}$ Collisions

F. Abe,[17] H. Akimoto,[36] A. Akopian,[31] M. G. Albrow,[7] S. R. Amendolia,[27] D. Amidei,[20] J. Antos,[33] S. Aota,[36] G. Apollinari,[31] T. Asakawa,[36] W. Ashmanskas,[18] M. Atac,[7] F. Azfar,[26] P. Azzi-Bacchetta,[25] N. Bacchetta,[25] W. Badgett,[20] S. Bagdasarov,[31] M. W. Bailey,[22] J. Bao,[39] P. de Barbaro,[30] A. Barbaro-Galtieri,[18] V. E. Barnes,[29] B. A. Barnett,[15] M. Barone,[9] E. Barzi,[9] G. Bauer,[19] T. Baumann,[11] F. Bedeschi,[27] S. Behrends,[3] S. Belforte,[27] G. Bellettini,[27] J. Bellinger,[38] D. Benjamin,[35] J. Benlloch,[19] J. Bensinger,[3] D. Benton,[26] A. Beretvas,[7] J. P. Berge,[7] J. Berryhill,[5] S. Bertolucci,[9] S. Bettelli,[27] B. Bevensee,[26] A. Bhatti,[31] K. Biery,[7] M. Binkley,[7] D. Bisello,[25] R. E. Blair,[1] C. Blocker,[3] A. Bodek,[30] W. Bokhari,[19] V. Bolognesi,[2] G. Bolla,[29] D. Bortoletto,[29] J. Boudreau,[28] L. Breccia,[2] C. Bromberg,[21] N. Bruner,[22] E. Buckley-Geer,[7] H. S. Budd,[30] K. Burkett,[20] G. Busetto,[25] A. Byon-Wagner,[7] K. L. Byrum,[1] J. Cammerata,[15] C. Campagnari,[7] M. Campbell,[20] A. Caner,[27] W. Carithers,[18] D. Carlsmith,[38] A. Castro,[25] D. Cauz,[27] Y. Cen,[30] F. Cervelli,[27] K. M. Chan,[30] P. S. Chang,[33] P. T. Chang,[33] H. Y. Chao,[33] J. Chapman,[20] M. -T. Cheng,[33] G. Chiarelli,[27] T. Chikamatsu,[36] C. N. Chiou,[33] L. Christofek,[13] S. Cihangir,[7] A. G. Clark,[10] M. Cobal,[27] E. Cocca,[27] M. Contreras,[5] J. Conway,[32] J. Cooper,[7] M. Cordelli,[9] C. Couyoumtzelis,[10] D. Crane,[1] D. Cronin-Hennessy,[6] R. Culbertson,[5] T. Daniels,[19] F. DeJongh,[7] S. Delchamps,[7] S. Dell'Agnello,[27] M. Dell'Orso,[27] R. Demina,[7] L. Demortier,[31] M. Deninno,[2] P. F. Derwent,[7] T. Devlin,[32] J. R. Dittmann,[6] S. Donati,[27] J. Done,[34] T. Dorigo,[25] A. Dunn,[20] N. Eddy,[20] K. Einsweiler,[18] J. E. Elias,[7] R. Ely,[18] E. Engels, Jr.,[28] D. Errede,[13] S. Errede,[13] Q. Fan,[30] G. Feild,[39] C. Ferretti,[27] I. Fiori,[2] B. Flaugher,[7] G. W. Foster,[7] M. Franklin,[11] M. Frautschi,[35] J. Freeman,[7] J. Friedman,[19] H. Frisch,[5] Y. Fukui,[17] S. Funaki,[36] S. Galeotti,[27] M. Gallinaro,[26] O. Ganel,[35] M. Garcia-Sciveres,[18] A. F. Garfinkel,[29] C. Gay,[11] S. Geer,[7] D. W. Gerdes,[15] P. Giannetti,[27] N. Giokaris,[31] P. Giromini,[9] G. Giusti,[27] L. Gladney,[26] D. Glenzinski,[15] M. Gold,[22] J. Gonzalez,[26] A. Gordon,[11] A. T. Goshaw,[6] Y. Gotra,[25] K. Goulianos,[31] H. Grassmann,[27] L. Groer,[32] C. Grosso-Pilcher,[5] G. Guillian,[20] R. S. Guo,[33] C. Haber,[18] E. Hafen,[19] S. R. Hahn,[7] R. Hamilton,[11] R. Handler,[38] R. M. Hans,[39] F. Happacher,[9] K. Hara,[36] A. D. Hardman,[29] B. Harral,[26] R. M. Harris,[7] S. A. Hauger,[6] J. Hauser,[4] C. Hawk,[32] E. Hayashi,[36] J. Heinrich,[26] B. Hinrichsen,[14] K. D. Hoffman,[29] M. Hohlmann,[5] C. Holck,[26] R. Hollebeek,[26] L. Holloway,[13] S. Hong,[20] G. Houk,[26] P. Hu,[28] B. T. Huffman,[28] R. Hughes,[23] J. Huston,[21] J. Huth,[11] J. Hylen,[7] H. Ikeda,[36] M. Incagli,[27] J. Incandela,[7] G. Introzzi,[27] J. Iwai,[36] Y. Iwata,[12] H. Jensen,[7] U. Joshi,[7] R. W. Kadel,[18] E. Kajfasz,[25] H. Kambara,[10] T. Kamon,[34] T. Kaneko,[36] K. Karr,[37] H. Kasha,[39] Y. Kato,[24] T. A. Keaffaber,[29] K. Kelley,[19] R. D. Kennedy,[7] R. Kephart,[7] P. Kesten,[18] D. Kestenbaum,[11] H. Keutelian,[7] F. Keyvan,[4] B. Kharadia,[13] B. J. Kim,[30] D. H. Kim,[7,*] H. S. Kim,[14] S. B. Kim,[20] S. H. Kim,[36] Y. K. Kim,[18] L. Kirsch,[3] P. Koehn,[23] K. Kondo,[36] J. Konigsberg,[8] S. Kopp,[5] K. Kordas,[14] A. Korytov,[8] W. Koska,[7] E. Kovacs,[7,*] W. Kowald,[6] M. Krasberg,[20] J. Kroll,[7] M. Kruse,[30] T. Kuwabara,[36] S. E. Kuhlmann,[1] E. Kuns,[32] A. T. Laasanen,[29] S. Lami,[27] S. Lammel,[7] J. I. Lamoureux,[3] M. Lancaster,[18] M. Lanzoni,[27] G. Latino,[27] T. LeCompte,[1] S. Leone,[27] J. D. Lewis,[7] P. Limon,[7] M. Lindgren,[4] T. M. Liss,[13] J. B. Liu,[30] Y. C. Liu,[33] N. Lockyer,[26] O. Long,[26] C. Loomis,[32] M. Loreti,[25] J. Lu,[34] D. Lucchesi,[27] P. Lukens,[7] S. Lusin,[38] J. Lys,[18] K. Maeshima,[7] A. Maghakian,[31] P. Maksimovic,[19] M. Mangano,[27] J. Mansour,[21] M. Mariotti,[25] J. P. Marriner,[7] A. Martin,[39] J. A. J. Matthews,[22] R. Mattingly,[19] P. McIntyre,[34] P. Melese,[31] A. Menzione,[27] E. Meschi,[27] S. Metzler,[26] C. Miao,[20] T. Miao,[7] G. Michail,[11] R. Miller,[21] H. Minato,[36] S. Miscetti,[9] M. Mishina,[17] H. Mitsushio,[36] T. Miyamoto,[36] S. Miyashita,[36] N. Moggi,[27] Y. Morita,[17] A. Mukherjee,[7] T. Muller,[16] P. Murat,[27] H. Nakada,[36] I. Nakano,[36] C. Nelson,[7] D. Neuberger,[16] C. Newman-Holmes,[7] C-Y. P. Ngan,[19] M. Ninomiya,[36] L. Nodulman,[1] S. H. Oh,[6] K. E. Ohl,[39] T. Ohmoto,[12] T. Ohsugi,[12] R. Oishi,[36] M. Okabe,[36] T. Okusawa,[24] R. Oliveira,[26] J. Olsen,[38] C. Pagliarone,[27] R. Paoletti,[27] V. Papadimitriou,[35] S. P. Pappas,[39] N. Parashar,[27] S. Park,[7] A. Parri,[9] J. Patrick,[7] G. Pauletta,[27] M. Paulini,[18] A. Perazzo,[27] L. Pescara,[25] M. D. Peters,[18] T. J. Phillips,[6] G. Piacentino,[27] M. Pillai,[30] K. T. Pitts,[7] R. Plunkett,[7] L. Pondrom,[38] J. Proudfoot,[1] F. Ptohos,[11] G. Punzi,[27] K. Ragan,[14] D. Reher,[18] A. Ribon,[25] F. Rimondi,[2] L. Ristori,[27] W. J. Robertson,[6] T. Rodrigo,[27] S. Rolli,[37] J. Romano,[5] L. Rosenson,[19] R. Roser,[13] T. Saab,[14] W. K. Sakumoto,[30] D. Saltzberg,[5] A. Sansoni,[9] L. Santi,[27] H. Sato,[36] P. Schlabach,[7] E. E. Schmidt,[7] M. P. Schmidt,[39] A. Scribano,[27] S. Segler,[7] S. Seidel,[22] Y. Seiya,[36] G. Sganos,[14] M. D. Shapiro,[18] N. M. Shaw,[29] Q. Shen,[29] P. F. Shepard,[28] M. Shimojima,[36] M. Shochet,[5] J. Siegrist,[18] A. Sill,[35] P. Sinervo,[14] P. Singh,[28] J. Skarha,[15] K. Sliwa,[37] F. D. Snider,[15] T. Song,[20] J. Spalding,[7] T. Speer,[10] P. Sphicas,[19] F. Spinella,[27] M. Spiropulu,[11] L. Spiegel,[7] L. Stanco,[25] J. Steele,[38] A. Stefanini,[27] J. Strait,[7] R. Ströhmer,[7,*] D. Stuart,[7] G. Sullivan,[5] K. Sumorok,[19] J. Suzuki,[36] T. Takada,[36] T. Takahashi,[24] T. Takano,[36] K. Takikawa,[36] N. Tamura,[12] B. Tannenbaum,[22] F. Tartarelli,[27] W. Taylor,[14] P. K. Teng,[33] Y. Teramoto,[24] S. Tether,[19] D. Theriot,[7] T. L. Thomas,[22] R. Thun,[20] R. Thurman-Keup,[1] M. Timko,[37] P. Tipton,[30] A. Titov,[31] S. Tkaczyk,[7] D. Toback,[5]

K. Tollefson,[30] A. Tollestrup,[7] H. Toyoda,[24] W. Trischuk,[14] J. F. de Troconiz,[11] S. Truitt,[20] J. Tseng,[19] N. Turini,[27] T. Uchida,[36] N. Uemura,[36] F. Ukegawa,[26] G. Unal,[26] J. Valls,[7,*] S. C. van den Brink,[28] S. Vejcik, III,[20] G. Velev,[27] R. Vidal,[7] R. Vilar,[7,*] M. Vondracek,[13] D. Vucinic,[19] R. G. Wagner,[1] R. L. Wagner,[7] J. Wahl,[5] N. B. Wallace,[27] A. M. Walsh,[32] C. Wang,[6] C. H. Wang,[33] J. Wang,[5] M. J. Wang,[33] Q. F. Wang,[31] A. Warburton,[14] T. Watts,[32] R. Webb,[34] C. Wei,[6] H. Wenzel,[16] W. C. Wester, III,[7] A. B. Wicklund,[1] E. Wicklund,[7] R. Wilkinson,[26] H. H. Williams,[26] P. Wilson,[5] B. L. Winer,[23] D. Winn,[20] D. Wolinski,[20] J. Wolinski,[21] S. Worm,[22] X. Wu,[10] J. Wyss,[25] A. Yagil,[7] W. Yao,[18] K. Yasuoka,[36] Y. Ye,[14] G. P. Yeh,[7] P. Yeh,[33] M. Yin,[6] J. Yoh,[7] C. Yosef,[21] T. Yoshida,[24] D. Yovanovitch,[7] I. Yu,[7] L. Yu,[22] J. C. Yun,[7] A. Zanetti,[27] F. Zetti,[27] L. Zhang,[38] W. Zhang,[26] and S. Zucchelli[2]

(CDF Collaboration)

[1] *Argonne National Laboratory, Argonne, Illinois 60439*

[2] *Istituto Nazionale di Fisica Nucleare, University of Bologna, I-40127 Bologna, Italy*

[3] *Brandeis University, Waltham, Massachusetts 02264*

[4] *University of California at Los Angeles, Los Angeles, California 90024*

[5] *University of Chicago, Chicago, Illinois 60638*

[6] *Duke University, Durham, North Carolina 28708*

[7] *Fermi National Accelerator Laboratory, Batavia, Illinois 60510*

[8] *University of Florida, Gainesville, Florida 33611*

[9] *Laboratori Nazionali di Frascati, Istituto Nazionale di Fisica Nucleare, I-00044 Frascati, Italy*

[10] *University of Geneva, CH-1211 Geneva 4, Switzerland*

[11] *Harvard University, Cambridge, Massachusetts 02138*

[12] *Hiroshima University, Higashi-Hiroshima 724, Japan*

[13] *University of Illinois, Urbana, Illinois 61801*

[14] *Institute of Particle Physics, McGill University, Montreal H3A 2T8, and University of Toronto, Toronto M5S 1A7, Canada*

[15] *The Johns Hopkins University, Baltimore, Maryland 21218*

[16] *Institut für Experimetelle Kernphysik, Universität Karlsruhe, 76128 Karlsruhe, Germany*

[17] *National Laboratory for High Energy Physics (KEK), Tsukuba, Ibaraki 315, Japan*

[18] *Ernest Orlando Lawrence Berkeley National Laboratory, Berkeley, California 94720*

[19] *Massachusetts Institute of Technology, Cambridge, Massachusetts 02139*

[20] *University of Michigan, Ann Arbor, Michigan 48109*

[21] *Michigan State University, East Lansing, Michigan 48824*

[22] *University of New Mexico, Albuquerque, New Mexico 87132*

[23] *The Ohio State University, Columbus, Ohio 43320*

[24] *Osaka City University, Osaka 588, Japan*

[25] *Universita di Padova, Istituto Nazionale di Fisica Nucleare, Sezione di Padova, I-36132 Padova, Italy*

[26] *University of Pennsylvania, Philadelphia, Pennsylvania 19104*

[27] *Istituto Nazionale di Fisica Nucleare, University and Scuola Normale Superiore of Pisa, I-56100 Pisa, Italy*

[28] *University of Pittsburgh, Pittsburgh, Pennsylvania 15270*

[29] *Purdue University, West Lafayette, Indiana 47907*

[30] *University of Rochester, Rochester, New York 14628*

[31] *Rockefeller University, New York, New York 10021*

[32] *Rutgers University, Piscataway, New Jersey 08854*

[33] *Academia Sinica, Taipei, Taiwan 11530, Republic of China*

[34] *Texas A&M University, College Station, Texas 77843*

[35] *Texas Tech University, Lubbock, Texas 79409*

[36] *University of Tsukuba, Tsukuba, Ibaraki 315, Japan*

[37] *Tufts University, Medford, Massachusetts 02155*

[38] *University of Wisconsin, Madison, Wisconsin 53806*

[39] *Yale University, New Haven, Connecticut 06511*

If quarks and leptons are composite and have a common substructure, the dilepton mass spectrum in $p\bar{p} \rightarrow l^+l^- + X$ interactions will show an excess at high masses relative to the standard model expectation. A search for such phenomena, using dielectrons (ee) and dimuons ($\mu\mu$) in 110 pb^{-1} of data collected with the Collider Detector at Fermilab, finds no significant deviations from the standard model. Assuming a contact interaction, limits on chiral quark-electron and quark-muon compositeness scales in the range of 2.5 to 4.2 TeV are obtained.

PACS numbers: 13.85Qk, 12.60Rc

In hadron-hadron collisions at high energies, massive lepton pairs are produced via the Drell-Yan [1] process, where pointlike quarks and antiquarks annihilate to form the dileptons. Experimentally, the process is distinctive: the leptons are well separated from jets of hadrons and other particles from the collision. In the standard model, the annihilation proceeds via a virtual photon or Z boson. If quarks and leptons have a common substructure, their constituents can interact. This new physics would add another amplitude to dilepton production and produce a deviation from the standard model prediction of the dilepton invariant mass spectrum.

At collision energies far below the mass scale of new physics, the new physics can be described by an effective four-fermion contact interaction. In this Letter, the contact Lagrangian [2] for first generation quarks $Q \equiv (u, d)$ and leptons $E \equiv (\nu_e, e)$ is

$$\begin{aligned}\mathcal{L}_{EQ} = {} & \xi^0_{LL}(\overline{E}_L\gamma_\mu E_L)(\overline{Q}_L\gamma^\mu Q_L) + \\ & \xi^1_{LL}(\overline{E}_L\gamma_\mu \tau_a E_L)(\overline{Q}_L\gamma^\mu \tau_a Q_L) + \\ & \xi^u_{LR}(\overline{E}_L\gamma_\mu E_L)(\overline{u}_R\gamma^\mu u_R) + \\ & \xi^d_{LR}(\overline{E}_L\gamma_\mu E_L)(\overline{d}_R\gamma^\mu d_R) + \\ & \xi^e_{RL}(\overline{e}_R\gamma_\mu e_R)(\overline{Q}_L\gamma^\mu Q_L) + \\ & \xi^u_{RR}(\overline{e}_R\gamma_\mu e_R)(\overline{u}_R\gamma^\mu u_R) + \\ & \xi^d_{RR}(\overline{e}_R\gamma_\mu e_R)(\overline{d}_R\gamma^\mu d_R) + \\ & \{[\xi^u_{SC}(\overline{e}_R e_L)(-\overline{u}_R u_L) + \\ & \xi^d_{SC}(\overline{e}_R e_L)(\overline{d}_L d_R)] + \text{h.c.}\},\end{aligned}$$

where $L(R)$ denotes the left(right)-helicity projection, SC denotes the scalar channel, and τ_a are Pauli matrices. The interaction strengths are $\xi_{ij} = \pm g_0^2/\Lambda_{ij}^2$, where Λ_{ij} is a mass (compositeness) scale, g_0 is an effective coupling, and $ij = LL, LR, \cdots$. Units of $\hbar = c = 1$ are used.

The dimuon and dielectron invariant mass spectra of $p\bar{p}$ collisions at a center-of-momentum energy of 1.8 TeV are from 110 pb^{-1} of collisions taken by the Collider Detector at Fermilab (CDF) during the 1992-95 collider runs.

CDF [3] is a solenoidal magnetic spectrometer surrounded by projective-tower-geometry calorimeters and outer muon detectors. Charged particle momenta and directions are measured by the spectrometer, which consists of a 1.4 T axial magnetic field, an 84 layer cylindrical drift chamber (CTC), and a vertex tracking chamber (VTX). The $p\bar{p}$ collision point along the beam line is determined using tracks in the VTX. When tracks are constrained to originate from the beam line, the momentum resolution is $\delta P_T/P_T^2 \simeq 0.001$, with P_T in GeV. For $P_T \lesssim 300$ GeV, the charge is well determined. The leptons are reconstructed and identified via the CTC, the central electromagnetic (CEM) and hadronic calorimeters, the shower maximum strip detector within the CEM calorimeter, and the muon detectors. The CEM calorimeter resolution is $(\delta E/E)^2 = 0.135^2/E_T + 0.017^2$, with E_T in GeV.

A three-level trigger [4] selects events containing electrons and muons. The final lepton selection closely parallels the dilepton selection of the CDF top-quark analysis [5]. The leptons of selected pairs have opposite charge and are both isolated from other activity in the calorimeters. The isolation is characterized by I_{cal}, the sum of transverse energy in the towers within a cone of radius 0.4 (in $\eta - \phi$ space) centered on the lepton, but excluding the towers containing the muon or the electron shower. Electrons of selected e^+e^- pairs have CTC tracks that extrapolate to fiducial shower clusters with $|\eta| < 1$ and $E_T > 20$ GeV in the CEM calorimeter. One electron must satisfy the trigger requirements. The dielectron invariant mass is calculated using the calorimeter energy ($|\vec{P}| = E$) and the track direction. In selected $\mu^+\mu^-$ pairs, one muon has $P_T > 20$ GeV, a matching track in the fiducial region of a muon detector, $|\eta| < 0.6$, and satisfies the trigger requirements; the other muon has $P_T > 17$ GeV, track hits in three of the five axial superlayers of the CTC [3], and $|\eta| < 1.2$. Cosmic ray muons are removed using tracking and calorimeter timing cuts. The dielectron selection, isolation, and trigger efficiencies are $(75 \pm 1)\%$, $(95 \pm 1)\%$, and $(99 \pm 1)\%$, respectively. The corresponding dimuon efficiencies are $(75 \pm 2)\%$, $(96 \pm 1)\%$, and $(76 \pm 3)\%$.

The dilepton invariant mass (M) distributions are shown in Table I. The cosmic ray background is negligible: 0.4 events overall and 0.03 events for $M > 150$ GeV. Charge symmetric backgrounds (e.g. from QCD jets) are estimated using same-charge lepton pairs. There are five dielectron and two dimuon same-charge lepton pairs, all with $M < 150$ GeV. Backgrounds from W^+W^-, $\tau^+\tau^-$, $c\bar{c}$, $b\bar{b}$, and $t\bar{t}$ sources are estimated using oppositely charged $e\mu$ pairs [6]. There are 36 $e\mu$ events, all with $M < 150$ GeV. These backgrounds are subtracted.

The lepton-pair cross section, $d^2\sigma/dMdy$, where y is the rapidity of the pair and the cross section is averaged over $|y| < 1$, is calculated in the leading-logarithmic QCD approximation with the CTEQ3L [7] parton distribution functions. The amplitudes from the Lagrangian, $\mathcal{L}_{EQ}$, are combined with the standard model amplitudes to calculate the cross sections used to determine the compositeness scale. A multiplicative "K-factor" is used to include higher order QCD corrections: $K(M^2) = 1 + \frac{4}{3}(1 + \frac{4}{3}\pi^2)\alpha_s(M^2)/2\pi$, where α_s is the second order QCD coupling. For $M > 50$ GeV, the factor brings the cross section to within 4% of the next-to-leading-logarithmic (NLL) QCD calculation. Above 90 GeV, the difference is less than 1%.

To establish compositeness scales, any deviation of the data from a prediction based on just the standard model is assumed to be due to composite fermions. The compositeness scale is defined using $g_0^2/4\pi = 1$. Each channel of $\mathcal{L}_{EQ}$, LL, LR, RL, RR, and SC, is tested one at a time. The interaction strengths are assumed to be quark flavor symmetric: $\xi^1_{LL} = 0$, $\xi^u_{LR} = \xi^d_{LR}$, $\xi^u_{RR} = \xi^d_{RR}$, and

$\xi^u_{SC} = \xi^d_{SC}$. Vector ($\xi_{SC} = 0$, $\xi_{LL} = \xi_{LR} = \xi_{RL} = \xi_{RR}$) and axial ($\xi_{SC} = 0$, $\xi_{LL} = -\xi_{LR} = -\xi_{RL} = \xi_{RR}$) current interactions, denoted as VV and AA, respectively, are also considered. The higher generation of quarks are incorporated into $\mathcal{L}_{EQ}$ by assuming symmetry among the generations. Muons are assumed to have the same interaction structure as the electrons.

Figure 1 shows the measured dilepton cross section compared against calculations. The composite fermion model cross sections are functions of the signed interaction strength, $\beta = \xi_{ij}/g_0^2 = \pm 1/(\Lambda^{\pm}_{ij})^2$:

$$\frac{d^2\sigma_{ij}(\beta)}{dMdy} = \frac{d^2\sigma_{SM}}{dMdy} + F^I_{ij}\,\beta + F^C_{ij}\,\beta^2,$$

where $ij = LL, LR, RL, \cdots$ (the compositeness model), $d^2\sigma_{SM}/dMdy$ is the standard model cross section, and the F^I_{ij} and F^C_{ij} are the interference and pure contact term coefficients, respectively. In $\Lambda^{\pm}_{ij}$, the $\pm$ refers to the sign of β. The parameter β gives the level of compositeness, with the standard model being $\beta = 0$.

The observed numbers of events for $M > 150$ GeV in Table I are compared against model predictions using a binned likelihood, $L_{ij}(\beta) \equiv \prod_k P_k(n, \mu_{ij}(\beta))$, where the product over k runs over the mass bins, and P_k is the Poisson probability of observing n events in bin k with an expected mean of $\mu_{ij}(\beta)$. The expected mean is $\mu_{ij}(\beta) = \sigma_{ij}(\beta)\mathcal{L}A\epsilon$, where $\sigma_{ij}(\beta)$ is the calculated bin cross section for $|y| < 1$, $\mathcal{L}$ the integrated luminosity, A the acceptance for $|y| < 1$, and ϵ the experimental efficiency. Detector resolution and QED final state radiative effects are included in $A\epsilon$. For $M > 110$ GeV, the standard model acceptance for either electrons or muons is greater than 24%. The predictions are normalized to the data over the Z resonance region of $50 < M < 150$ GeV. This removes the dependence on the value of $\mathcal{L}$ and reduces the dependence on the systematic errors of $A\epsilon$.

The dielectrons and dimuons are compared separately to model predictions. Figure 2 shows the likelihood functions for the LL model. Standard model predictions for the number of expected dielectrons and dimuons are given in Table I. No significant discrepancy from the standard model is observed. The confidence interval in the β parameter of each model is derived from the probability density,

$$f_{ij}(\beta) = L_{ij}(\beta) \;/ \int_{-\infty}^{+\infty} L_{ij}(\beta')d\beta'.$$

The lower limits on the quark-electron (qe), quark-muon ($q\mu$) compositeness scales, and quark-lepton scales assuming lepton universality (combined likelihood) are given in Table II. The mean and rms from each probability density, f_{ij}, are listed under $<\beta>$. The SC channel limits are not stringent as those from its charged current counterpart, which is strongly constrained by $e\mu$ universality in pion decays [10]. In the chiral channels, Λ_{qe} and $\Lambda_{q\mu}$ range from 2.5 to 4.2 TeV. In previous searches, the limits have ranges of 1.4 to 2.2 TeV in $p\bar{p}$ [11] collisions, 1.6 to 2.5 TeV in e^+e^- [12] collisions, and 1.0 to 2.5 TeV in ep [13] collisions. In comparison, quark-quark [14] and neutrino-quark [15] compositeness scale limits range from 1.6 to 1.8 TeV and 1.3 to 5.2 TeV, respectively.

The results in Table II are based on the assumption that leptons couple symmetrically to u-type (u, c, t) and d-type (d, s, b) quarks. Alternatively, Table III gives limits based on the assumption that leptons couple only to u-type quarks or only to d-type quarks.

Another way of investigating possible quark and lepton substructure is with form factors [16]. Deviations from the standard model cross section are parametrized as

$$\frac{d^2\sigma}{dMdy} = \frac{d^2\sigma_{SM}}{dMdy} f_q^2(M^2) f_l^2(M^2),$$

where $f(M^2) = 1 + \frac{1}{6}R^2M^2$ is a Dirac form factor for quarks (q) and leptons (l), and R^2 is the mean-square radius of the quark or lepton if the γ^*/Z bosons are assumed to be pointlike. Assuming $f_q = f_l$, the likelihood analysis on the combined dielectron and dimuon data gives $R < 5.6 \times 10^{-17}$ cm at the 95% confidence level limit. A similar analysis from ep collisions gives $R < 26 \times 10^{-17}$ cm [13]. A complementary analysis of anomalous magnetic moments using e^+e^- collider Z resonance data gives $R < 10^{-17}$ cm [16].

In conclusion, this search for quark-lepton substructure in $p\bar{p} \to e^+e^-, \mu^+\mu^- + X$ interactions finds no significant deviation from the standard model. The contact interaction analysis yields improved limits on the qe and $q\mu$ compositeness scales. The scales are comparable within the chiral channels, with Λ^+ in the range of 2.5–3.2 TeV and Λ^- in the range of 3.2–4.2 TeV. The AA and VV model limits are more stringent, with Λ in the range of 3.5–6.0 TeV. The form factor analysis on a common quark and lepton size yields $R < 5.6 \times 10^{-17}$ cm.

The vital contributions of the Fermilab staff and the technical staffs of the participating institutions are gratefully acknowledged. This work is supported by the U.S. Department of Energy and National Science Foundation, the Italian Istituto Nazionale di Fisica Nucleare, the Ministry of Education, Science and Culture of Japan, the Natural Sciences and Engineering Research Council of Canada, the National Science Council of the Republic of China, the A.P. Sloan Foundation, and the Swiss National Science Foundation.

---

* Visitor.

[1] S.D. Drell and T.-M. Yan, Phys. Rev. Lett. **25**, 316 (1970).

[2] E.J. Eichten, K.D. Lane, M.E. Peskin, Phys. Rev. Lett. **50**, 811 (1983); E. Eichten, I. Hinchliffe, K. Lane, C. Quigg, Rev. Mod. Phys. **56**, 579 (1984); T. Lee, Phys. Rev. D **55**, 2591 (1997).
[3] F. Abe *et al.*, Nucl. Instrum. and Methods in Phys. Res. Sect. A **271**, 387 (1988). The CDF coordinate system uses (θ, ϕ), where θ is the polar angle relative to the proton beam, and ϕ the azimuth. The pseudorapidity is $\eta = -\ln\tan(\theta/2)$. The transverse momentum of a particle is $P_T = P\sin\theta$. The transverse energy is $E_T = E\sin\theta$, where E is the energy measured in the calorimeter.
[4] F. Abe *et al.*, Phys. Rev. D **50**, 2966 (1994).
[5] The cuts are similar to the top analysis [4] cuts, with isolation $I_{cal} < 4$ GeV if $M < 110$ GeV, else $I_{cal} < 0.1 \times (E_T(e)$ or $P_T(\mu))$, and with electron $(E/P)_{strict} < 1.8$ and $\chi^2_{strip} < 10$.
[6] The CDF top-quark high-P_T dilepton selection [4] is used, but with both leptons isolated and no jet cuts.
[7] H.L. Lai *et al.*, Phys. Rev. D **51**, 4763 (1995).
[8] F. Abe *et al.*, Phys. Rev. D **49**, 1 (1994); F. Abe *et al.*, Phys. Rev. Lett. **76**, 3070 (1996).
[9] P.J. Sutton *et al.*, Phys. Rev. D **45**, 2349 (1992); A.D. Martin *et al.*, Phys. Lett. B **354**, 155 (1995). $\overline{\text{MS}}$ with MRS-A$'$ nucleon parton distribution functions.
[10] O. Shanker, Nucl. Phys. B **204**, 375 (1982).
[11] F. Abe *et al.*, Phys. Rev. Lett. **67**, 2418 (1991); F. Abe *et al., ibid.* **68**, 1463 (1992).
[12] G. Alexander *et al.*, Phys. Lett. B **387**, 432 (1996).
[13] S. Aid *et al.*, Phys. Lett. B **353**, 578 (1995).
[14] F. Abe *et al.*, Phys. Rev. Lett. **77**, 5336 (1996).
[15] K.S. McFarland *et al.*, FERMILAB-PUB-97/001-E.
[16] G. Köpp *et al.*, Z. Phys. C **65**, 545 (1995).

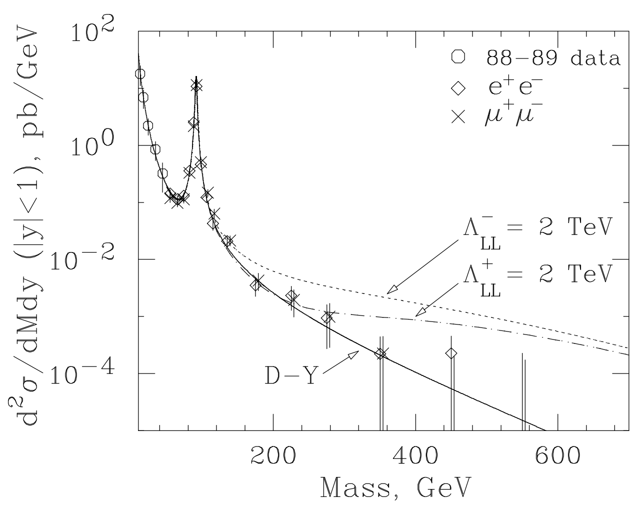

FIG. 1. $d^2\sigma/dMdy$, $|y| < 1$ for $p\bar{p} \to l^+l^- + X$. The circles ($M < 50$ GeV) are from earlier data [8]; the diamonds and crosses are the dielectron and dimuon data, repectively, normalized from 50 to 150 GeV to the standard model value. Above 110 GeV, the data symbols are displaced for clarity. The D-Y curve is a standard model NLL calculation [9]. Superimposed are LL model calculations with $\Lambda = 2$ TeV.

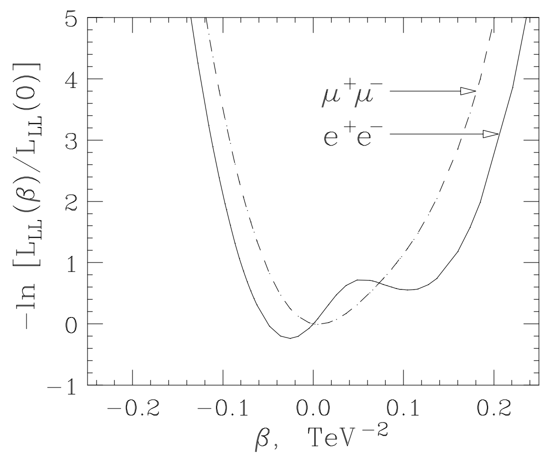

FIG. 2. Negative logarithms of the LL model likelihoods. The solid (dashed) curve is for the dielectrons (dimuons). The standard model corresponds to $\beta = 0$.

TABLE I. The dilepton event samples. The SM columns are the standard model event predictions normalized to the data over 50-150 GeV. There are no events above 500 GeV.

Mass Bin (GeV)	Dielectrons Data	Dielectrons SM	Dimuons Data	Dimuons SM
50-150	2581	$\equiv$ 2581	2533	$\equiv$ 2533
150-200	8	10.8	9	9.7
200-250	5	3.5	4	3.2
250-300	2	1.4	2	1.3
300-400	1	0.97	1	0.94
400-500	1	0.25	0	0.27
500-600	0	0.069	0	0.087

TABLE II. The one-sided 95% confidence level lower limits of the compositeness scales from $f_{ij}(\beta)$. The Λ^+ is from the $\beta > 0$ side (+ interference structure) and the Λ^- is from the $\beta < 0$ side (− interference structure). The $<\beta>$ entry gives the mean value of $f_{ij}(\beta)$ ($< \pm 1/\Lambda^2 >$) and its rms. The last three columns give the combined results.

Model ij	Λ^+_{qe} TeV	Λ^-_{qe} TeV	$<\beta_{qe}>$ TeV^{-2}	$\Lambda^+_{q\mu}$ TeV	$\Lambda^-_{q\mu}$ TeV	$<\beta_{q\mu}>$ TeV^{-2}	Λ^+ TeV	Λ^- TeV	$<\beta>$ TeV^{-2}
LL	2.5	3.7	0.026±0.075	2.9	4.2	0.023±0.053	3.1	4.3	0.009±0.047
LR	2.8	3.3	0.014±0.071	3.1	3.7	0.012±0.055	3.3	3.9	0.010±0.050
RL	2.9	3.2	0.009±0.070	3.2	3.5	0.008±0.055	3.3	3.7	0.006±0.050
RR	2.6	3.6	0.026±0.073	2.9	4.0	0.021±0.054	3.0	4.2	0.013±0.050
VV	3.5	5.2	0.008±0.036	4.2	6.0	0.010±0.025	5.0	6.3	0.001±0.020
AA	3.8	4.8	0.011±0.036	4.2	5.4	0.008±0.027	4.5	5.6	0.006±0.025
SC	2.9	2.9	0.000±0.077	3.1	3.1	0.000±0.061	3.3	3.3	0.000±0.055

TABLE III. The one-sided 95% confidence level lower limits of the compositeness scales in models where leptons couple only to u-type quarks (ue, $u\mu$) or to d-type quarks (de, $d\mu$).

Model ij	Λ^+_{ue} TeV	Λ^-_{ue} TeV	Λ^+_{de} TeV	Λ^-_{de} TeV	$\Lambda^+_{u\mu}$ TeV	$\Lambda^-_{u\mu}$ TeV	$\Lambda^+_{d\mu}$ TeV	$\Lambda^-_{d\mu}$ TeV
LL	2.9	3.7	2.3	1.6	3.4	4.1	2.3	1.7
RR	2.5	3.5	2.0	1.7	3.0	4.0	2.1	1.8
LR	2.7	3.2	1.9	1.8	3.0	3.6	2.0	1.9